

LATE AGB MAGNETIC CYCLES: MHD SOLUTIONS FOR THE HST PN RINGS

Guillermo García-Segura¹, José Alberto López², José Franco^{3,4}

Instituto de Astronomía-UNAM, Apdo Postal 877, Ensenada, 22830 Baja California,
Mexico

Received _____; accepted _____

¹Email address: ggs@astrosen.unam.mx

²Email address: jal@astrosen.unam.mx

³Instituto de Astronomía-UNAM, Apdo Postal 70-264, 04510 México D. F., Mexico

⁴Email address: pepe@astrocu.unam.mx

ABSTRACT

The Hubble Space Telescope has revealed the existence of multiple, regularly spaced, and faint concentric shells around some planetary nebulae. Here we present 2(1/2)D magnetohydrodynamic numerical simulations of the effects of a solar-like magnetic cycle, with periodic polarity inversions, in the slow wind of an AGB star. The stellar wind is modeled with a steady mass-loss at constant velocity. This simple version of a solar-like cycle, without mass-loss variations, is able to reproduce many properties of the observed concentric rings. The shells are formed by pressure oscillations, which drive compressions in the magnetized wind. These pressure oscillations are due to periodic variations in the field intensity. The periodicity of the shells, then, is simply a half of the magnetic cycle since each shell is formed when the magnetic pressure goes to zero during the polarity inversion. As a consequence of the steady mass-loss rate, the density of the shells scales as r^{-2} , and their surface brightness has a steeper drop-off, as observed in the shells of NGC 6543, the best documented case of these HST rings. Deviations from sphericity can be generated by changing the strength of the magnetic field. For sufficiently strong fields, a series of symmetric and equidistant blobs are formed at the polar axis, resembling the ones observed in He 2-90. These blobs are originated by magnetic collimation within the expanding AGB wind.

Subject headings: Hydrodynamics—ISM: Planetary Nebulae, jets and outflows, bubbles, —ISM: Individual (NGC 6543, Hb 5, He 2-90 , K 1-2)—Stars: AGB

1. Introduction

The multiple concentric rings, or arcs, that were recently discovered by the Hubble Space Telescope around a handful of planetary nebulae (PNe) is one of the most puzzling and unexpected results delivered by the HST (see Kwok, Su, & Hrivnak 1998; Hrivnak, Kwok & Su 2001; Terzian & Hajian 2000 and references therein). The best documented case of these systems of faint concentric rings (hereafter called HST rings) is displayed by NGC 6543 (Balick, Wilson & Hajian 2000). In reality, they are regularly spaced concentric shells, indicating quasi-periodic events with time intervals, assuming typical expansion velocities of AGB winds, in the range of 500 to 1500 years. These time scales are too short for thermal pulses and too long for acoustic envelope pulsations and, thus, the origin of the rings cannot be ascribed to any of this type of events. Soker (2000) made a critical review of the mechanisms that have been proposed to explain them, and he indicates that mass-loss variations associated with solar-like magnetic cycles are perhaps the best alternative for their origin.

In a more recent paper, Simis, Icke & Dominik (2001) discuss a new non-magnetic alternative, and present detailed 1D hydrodynamical simulations for the acceleration of a dusty AGB wind. They include dust grain nucleation and growth in the AGB atmosphere, and the dust and gas components are treated as two separated fluids, without assumptions about grain drift or dust-gas coupling. Recently formed grains are accelerated first and then, as they drift through the gas at relatively large speeds (sometimes well above the equilibrium drift velocity), the drag force transmits the momentum to the gas. For non-magnetic dusty flows, and depending on grain properties (*i. e.*, chemical composition, size, and charge) and local conditions (*i. e.*, ionization fraction and temperature), an efficient momentum transfer requires that the grains sweep through gas column densities of the order of $N \sim 10^{19} a_5 \text{ cm}^{-2}$ (where a_5 is the grain radius in units of 10^{-5} cm ; Franco *et al.*

1991). Thus, the grain drift velocity can be larger than its equilibrium value for a certain distance, compressing the gas at some locations and creating regions with larger dust-to-gas mass ratios. These compressions appear in a cyclic manner in their 1D simulations and, if such a flow configuration is stable in two or three dimensions, they can drive a variable mass loss rate and may lead to the creation of dusty shells. The stability of this process, however, is difficult to explore at the moment, and it is unclear if the compressions can truly create shells or if they only lead to inhomogeneities in these radiatively driven outflows. Thus, at present, one can consider that dusty flow oscillations (if they really exist) or solar-like magnetic cycles are two possible candidates to generate the HST rings.

In Soker’s (2000) view, the magnetic field plays no direct role in the evolution of the AGB wind, however temporal variation in the number of magnetic spots would be able to modify the mass-loss rate. The number of cool spots over the AGB surface, which could be preferred sites for dust formation, is controlled by the magnetic cycle. Thus, given that the mass-loss is driven by radiation pressure on dust grains, the same cycle may also regulate periodic variations in the mass-loss rate. In this interpretation, the magnetic field is a passive player with no dynamical effects, and the mass-loss rate simply follows the spot cycle activity. In addition, to make a logical association with bipolar PNe, he suggests that a stronger magnetic activity could be expected from dynamo amplification in binary systems.

Here we develop a different point of view and explore some of the actual dynamical effects of a solar-like magnetic cycle. The possibility of a solar-like magnetic dynamo at the AGB phase has been recently discussed by Blackman *et al.* (2001), and they conclude that dynamo amplification is likely to operate in rotating AGB stars. A logical extension of this result is that a solar-like activity, including dynamo and cycles, is also expected in some AGB stars. We thus build a very simple model, without mass-loss variations, and perform

2(1/2)D magnetohydrodynamic computations considering a cyclic polarity inversion of the surface magnetic field of an AGB star. Our results show the importance of MHD effects in the formation of the HST rings and successfully reproduce their main features. This indicates that modulated mass-loss episodes are not really necessary to generate the rings. In Section 2 we describe the MHD models and results. A brief discussion is given in Section 3.

2. Numerical Models

2.1. The Method

The simulations have been performed using the magnetohydrodynamic code ZEUS-3D (version 3.4), developed by M. L. Norman and the Laboratory for Computational Astrophysics. This is a finite-difference, fully explicit, Eulerian code descended from the code described in Stone & Norman (1992). A method of characteristics is used to compute magnetic fields, as described in Clarke (1996), and flux freezing is assumed in all the runs. We have used spherical polar coordinates (r, θ, Φ) , with reflecting boundary conditions at the equator and the polar axis. Rotational symmetry is assumed with respect to the rotational (polar) axis, and our models are effectively two-dimensional. The simulations are carried out in the meridional (r, θ) plane, but three independent components of the velocity and magnetic field are computed (*i. e.*, the simulations are “two and a half” dimensions). We are unable to include, as Simis *et al.* (2001) have done with their two-fluid code, the effects of dust in our simulations.

Our grids consist of 200×180 equidistant zones in r and θ , respectively (with a radial extent of 0.1 pc, and an angular extent of 90°), and the innermost radial zone lies at $r = 2.5 \times 10^{-3}$ pc from the central star. These values are used in all the simulations shown

in Figures 1 – 3.

The equations for the stellar wind flow are simple, since we model an isothermal, slow AGB wind with constant mass-loss rate ($10^{-6} M_{\odot} \text{ yr}^{-1}$) and radial velocity (10 km s^{-1}). These values represent the boundary conditions used in the first five innermost radial zones. Rotational effects are not important in these outflows, since we have used a small value for the stellar rotation velocity, 0.01 km s^{-1} (see García-Segura *et al.* 1999 for more details).

The novel aspect in this paper is the simple treatment of the stellar magnetic field (B_s), which it is allowed to change sign in a cycle of the form:

$$B_s(t) = B_{\text{max}} \cos\left(2\pi \frac{t}{P}\right), \quad (1)$$

where B_{max} is the maximum average B -field at the AGB surface, and P is the period of the magnetic cycle. Since we do not know the true variation form of the field, this functional form is just a first simple approximation. As in the case of the Sun, we assume that B_{max} has opposite signs at each hemisphere, with a neutral current sheet near the equatorial plane (*e. g.* Wilcox & Ness 1965; Smith, Tsurutani & Rosenberg 1978). Its average thickness in the solar case is of about 10^8 cm , and its presence does not affect the field outside the equatorial sections. For simplicity, given that we compute only one hemisphere, we neglect the size of this current sheet. The equation for the inner boundary wind toroidal field on the computational domain, which is restricted to one hemisphere ($0 \leq \theta < \pi/2$), is:

$$B_{\phi}(t) = B_s(t) \frac{v_{\text{rot}}}{v_{\infty}} \left(\frac{R_s}{r}\right)^2 \left(\frac{r}{R_s} - 1\right) \sin \theta, \quad (2)$$

where v_{rot} is the stellar rotation velocity, v_{∞} the wind velocity, and R_s the stellar radius. The function $\sin \theta$ cancels the toroidal component at the symmetry axis, $\theta = 0$ (pole). The poloidal field component can be neglected at large distances, so that our field configuration naturally satisfies the condition $\nabla \cdot B = 0$.

The parameter which identifies our models is the ratio of the magnetic field energy

density to the kinetic energy density in the wind (Begelman & Li 1992)

$$\sigma(t) = \frac{B^2}{4\pi\rho v_\infty^2} = \frac{B_s^2(t)R_s^2}{\dot{M} v_\infty} \left(\frac{v_{\text{rot}}}{v_\infty}\right)^2. \quad (3)$$

Obviously, this parameter is always positive and oscillates with twice the frequency of the stellar magnetic cycle.

2.2. Results

The first model, shown in Figure 1, corresponds to the case of a slow and dense wind ($v_\infty = 10 \text{ km s}^{-1}$ and $\dot{M} = 10^{-6}M_\odot \text{ yr}^{-1}$), in which the magnetic field at the surface of the AGB star cycles with a full period of 2000 yr. A peak value $\sigma_{\text{max}} = 0.01$ is used for a slowly rotating AGB star ($v_{\text{rot}} = 0.01 \text{ km s}^{-1}$), which is achieved, for example, when the star has $B_s = 53 \text{ G}$ and $R_s = 1 \text{ AU}$, or $B_s = 113 \text{ G}$ and $R_s = 100 R_\odot$. For the cases discussed by Soker (2000), $R_s = 2 \text{ AU}$ and $0.2 \text{ km s}^{-1} \leq v_{\text{rot}} \leq 2 \text{ km s}^{-1}$, the required surface magnetic fields are within $1.3 \text{ G} \geq B_s \geq 0.13 \text{ G}$. These field strength values are modest compared with the ones that could be achieved by dynamo amplification during AGB evolution (Blackman *et al.* 2001).

Figure 1 displays radial cuts, on the equatorial plane, of some of the wind variables at $t = 10,000 \text{ yr}$ after the onset of the magnetized wind. The first (top) panel shows the existence of equidistant concentric shells, separated by 1,000 yr, a half of the magnetic cycle period. Each density peak corresponds to a minimum in the magnetic pressure (second panel), which also occurs at the moment when the magnetic field changes polarity (fourth panel). The last panel of Figure 1 displays the radial velocity, which clearly shows the gas response to the local variations in the total pressure (third panel) of the wind.

Thus, shell formation in a magnetized wind with variable field strength is a straightforward process. The outflowing plasma notices the magnetic pressure depressions,

both upstream and downstream in the wind, and moves towards the low-pressure sites. The wind is then compressed at these locations, increasing the local density, to compensate for the low magnetic pressure values. Obviously, the particular values achieved at these density peaks, and the density contrast between ring and inter-ring zones, depend on the model assumptions. Thus, these values can be modified by changing the amplitude of the pressure fluctuations (*i. e.*, by changing the maximum field intensities, or adding mass-loss or velocity variations, etc.) but, for our purposes, it is sufficient to show that a reasonable density contrast is achieved by this simple model. The total pressure plot (third panel), shows that the local pressure fluctuations decrease with time (or position in the wind). As the plasma flows from the positions of the magnetic peaks and compresses the gas of the valleys, a series of MHD waves are continuously driven that maintains small gas oscillations in the expanding wind.

Figure 2 shows the emission measure of four different models, with $\sigma_{\max} = 0.001, 0.01, 0.05, 0.1$. The plots nicely reproduce the typical spacing of the rings, and show the general drop-off expected for a constant mass-loss wind. The structures are in reality a set of spherical or quasi-spherical hemispheric shells, and their projected maximum column densities in the plane of the sky give the impression of concentric rings. For large enough values of σ_{\max} , the magnetized AGB wind is able to self-collimate towards the polar axis. This self-collimation is also present in the free streaming fast winds that form some PNe (see García-Segura *et al.* 1999) but, given the large densities of the slow AGB winds, the self-collimated structures are particularly prominent, and easily observable features in this case. The two right panels in Figure 2 clearly show the resulting structures, that are better defined and more conspicuous in the $\sigma_{\max} = 0.1$ case. The self-collimated gaseous structures also follow the periodic variations of the magnetic field, resulting in two strings of regularly spaced blobs located along the polar axis resembling those observed in He 2-90 (Sahai & Nyman 2000).

3. Discussion and Summary

A relevant point for the applicability of this model is whether or not the B -field can be considered frozen into the outflowing dusty AGB wind, and if the simple MHD effects that we have described are truly operative during wind evolution. This question has been previously explored by several authors and in much more restrictive environments. For instance, in collapsing molecular clouds with ionization fractions as low as 10^{-7} , where ion drift could lead to substantial magnetic flux leakage. Nonetheless, even at these very low ionization fraction values, numerical models of cloud collapse show that the field remains nearly frozen into the cloud for long periods of time (*e. g.* Black & Scott 1982). For AGB winds the situation is certainly more favorable because the ions are provided by a number of species with low ionization potentials (Habing 1996; Cox 1997), and charged dust grains are also well coupled to the magnetic field of the outflow. Thus, flux leakage is not considered important during the AGB phase, which occurs during time scales of the order of 10^3 to 10^5 yr (for cases where ambipolar diffusion is important see Mac Low *et al.* 1995 and references therein). Later on, the AGB wind is photoionized by the central star of the PN (as in NGC 6543 or Hb 5), and the temperature and ionization fraction of the outflowing plasma is suddenly increased. Some pressure readjustments occur within the photoionized plasma at this time, but the basic shell structuring remains unchanged. Obviously, flux leakage becomes irrelevant after this moment, and the rings can survive for longer periods of time.

An important issue related with the validity of the present results is whether or not magnetic reconnection can occur in the flow, modifying some of the features appearing in the models. As stated before, in analogy with the solar case, it is likely that the general AGB B -field has a dipolar structure, and a neutral current sheet should be present around the equatorial plane of their magnetized winds. The process creates a pair of half-shells at each cycle, one per hemisphere and separated by the neutral current sheet at the

equatorial plane. Each half-shell, in turn, is compressed by magnetic intershell regions with opposite polarities. This implies that the compressed half shells also act as neutral current sheets, separating regions with oppositely directed field lines. Our simulations assume well ordered fields and the results do not show, even in the more magnetic models, any signs of reconnection within the shells. If one assumes that a twisted random field component could be also present, a faster reconnection mode could also occur (*e. g.* Lazarian & Vishniac 1999). Given the low field values in the shells, however, any random field reconnection that may occur within them is severely limited by the corresponding low Alfvén speeds, and the energy and flux involved in such a process has to be negligible.

Another related question is if the shells can be formed only by modulated mass-loss rate episodes, without magnetic pressure in the wind, as proposed by Soker (2000) and Simis *et al.* (2001) (keeping in mind that the Simis *et al.* results could be unstable in 2D or 3D, precluding the actual formation of a shell). In these cases, the periodic formation of shells in the expanding wind is only due to the increase in mass-loss, and the higher shell densities can be maintained as long as the wind temperature decreases in these same locations. This is a perfectly reasonable possibility during the AGB phase. However, once the wind becomes photoionized, the plasma temperature becomes fairly homogeneous, and the rings tend to be washed away in a sound crossing time. Thus, ring survival is severely compromised in these purely hydrodynamic cases.

There is one additional observational element that suggests that the magnetohydrodynamic mechanism is indeed relevant in these cases. Recent HST images of He 2-90 show a series of bright knots which have been interpreted as due to symmetric and well collimated fast jets (Sahai & Nyman 2000). New spectroscopic observations by Guerrero *et al.* (2001) have found that these jet-like features are moving away from He 2-90 at a remarkably constant radial velocity of only 26 km s^{-1} . Obviously,

this radial speed value has to be corrected for the inclination angle with respect to the plane of the sky. This angle is unknown, but assuming that the axis of the jet-like features is located almost on the plane of the sky, they find an upper bound to the actual space velocity of about 290 km s^{-1} . However, the lack of any trace of collisional excitation within the flow or interaction with the ambient medium (*i. e.*, the sulfur and oxygen lines in the collimated structures are weak, and there are no signs of the bow-shocks expected for the leading parts of supersonic jets), makes it difficult to ascribe these highly collimated structures with a supersonic jet (this is reinforced by the observed narrow line profiles and lack of acceleration within the structures). In contrast, the constant and moderate velocity values, and the similarity of the observed knotty structure with the largest σ_{\max} model presented here provides a very attractive alternative for its origin. Figure 3 shows a qualitative comparison of one of the models ($\sigma = 0.1$) with the structuring of the “jets” in He 2-90 (figure 3 in Sahai & Nyman 2000). As stated above, the peak densities depend on model assumptions and, despite the fact that we have not attempted to specifically reproduce this nebula, the similarity is outstanding. Thus, although the images actually show features that resemble supersonic, fast jets, their observed properties, and our model, indicate that these features could have a different nature. If this is the case, the velocity of the knots should be close to that of the AGB wind, and the low radial velocity observed by Guerrero *et al.* (2001) is compatible with our model.

Since jets are actually formed by magnetic collimation, the jet interpretation of Sahai & Nyman (2000) and Guerrero *et al.* (2001) has a logical link with our results, but there is one important difference. This key difference is that the gas in our case is *only* collimated but *not* accelerated. The collimation of these outflows is solely due to the hoop stress of the toroidal field, but their acceleration require an additional process. For instance, the acceleration of a jet-like flow in some planetaries is achieved after the magnetized wind passes through a reverse shock and then is subsequently pinched at the

polar axis (Różyczka & Franco 1996). The case of He 2-90 is probably different since, although magnetic collimation is most likely present, the acceleration mechanism to create a “supersonic fast jet” seems to be absent. Note that collimation without acceleration can occur in a freely outflowing magnetized wind.

It is also relevant to ask if the shells formed in our models are stable against the 2D undular or interchange modes, or the 3D mixed mode, of the Parker instability (the 3D mixed mode is a combination of the interchange and undular modes; see Hughes & Cattaneo 1987, and Matsumoto *et al.* 1993). The growth rates of these instabilities depend on the field strength, the acceleration of the magnetized plasma, and size of the magnetically supported regions, but the fastest growing mode corresponds to the interchange instability (in this case, the flux tubes are displaced in the radial direction, following the pressure gradient). The undular instability, on the other hand, grows at a slower pace and distorts the B -field lines, creating a wavy structure along the field lines. For the model configurations considered here, the simulations are blind to the undular instability (because this branch grows in a plane perpendicular to the computational domain; see Kim *et al.* 2000) but they should be able to resolve some modes (*i. e.*, those with wavelengths larger than the grid size) of the interchange instability. The accelerations of the flow, however, are very small and the resulting growth time scales are much too large. Thus, for any practical purposes, the models are effectively stable to these perturbances.

In addition, given that the higher pressure intershell regions become lighter than the shells, the growth of plain Rayleigh-Taylor instabilities in the radial direction could become relevant at some stage. Our simulations cannot resolve the fine scales of this instability, but a simple analysis indicates that the growth times are also large. One cannot define a sharp interface between the (magnetic) intershell and (non-magnetic) shell regions (their initial densities are equal), but the maximum pressure difference is simply equal to $B_{\max}^2/8\pi$.

Thus, for a shell thickness L , an upper limit to the pressure gradient in the radial direction is simply $B_{\max}^2/8\pi L$, and the corresponding upper limit to the acceleration during shell formation is $a \sim v_a^2/2L$ (where v_a is the average Alfvén speed inside the shell). The resulting growth time for R-T instabilities is then (Shore 1992),

$$\tau \sim \left(\frac{\rho_2 + \rho_1}{\rho_2 - \rho_1}\right)^{1/2} \left(\frac{L}{a}\right)^{1/2} \geq \left(\frac{\rho_2 + \rho_1}{\rho_2 - \rho_1}\right)^{1/2} \left(\frac{2^{1/2}L}{v_a}\right), \quad (4)$$

where ρ_2 is the shell density, and ρ_1 is the intershell density. Clearly, this time scale is always large: at the early stages because the density contrast is very small, and because the acceleration drops as the density difference grows at later stages. Thus, the growth time of RT instabilities is always larger than the time scale for shell formation.

In summary, the dynamical effects of a solar-like magnetic cycle operating in late AGB stars have been explored with MHD models. Although a number of simplifying assumptions have been made, these 2(1/2)D numerical simulations are able to successfully reproduce for the first time the main observed properties of the HST rings. One obvious limitation of our models is that we are unable to include the dynamical effects of dust grains, and cannot explore the magnetic counterpart of the Simis *et al.* (2001) models. Further studies with less restrictive assumptions may shed more light on the range of MHD effects that may operate in these type of objects.

Acknowledgments It is a pleasure to thank Yervant Terzian for his helpful discussions and encouragement about this topic during his visit to Ensenada. We also thank Jack Thomas for pointing out the recent work on dynamo amplification in AGB stars. We warmly thank M. Guerrero, L.F. Miranda, Y-H. Chu, M. Rodriguez and R.M. Williams for sharing their results with us prior to publication. The comments and criticisms of the referee are also gratefully acknowledged. As usual, we also thank Michael L. Norman and the Laboratory for Computational Astrophysics for the use of ZEUS-3D. The computations were performed at Instituto de Astronomía-UNAM. This work has been partially supported

by grants from DGAPA-UNAM (IN130698, IN117799 & IN114199) and CONACyT (32214-E).

List of References

- Balick, B., Wilson, J. & Hajian, A. R. 2000, *AJ*, 121, 354
- Begelman, M. & Li, Z. Y. 1992, *ApJ*, 397, 187
- Black, D. C. & Scott, E. H. 1982, *ApJ*, 263, 696
- Blackman, E. G., Frank, A., Markiel, J. A., Thomas, J. H. & Van Horn, H. M. 2001, *Nature*, 409, 485
- Clarke, D. A. 1996, *ApJ*, 457, 291
- Cox, P. 1997, in *IAU Symp. No 180 “Planetary Nebulae”*, eds. H. J. Habing & H. J. G. L. M. Lamers, (Kluwer Academic Publishers, Dordrecht), 139
- Franco, J., Ferrini, F., Ferrara, A. & Barsella, B. 1991, *ApJ*, 366, 443
- Habing, H. J. 1996, *A&A Rev.*, 7, 97
- Hrivnak, B. J., Kwok, S. & Su, K. Y. L. 2001, *AJ*, 121, 2775
- Hughes, D. W. & Cattaneo, F. 1987, *Geophys. Astrophys. Fluid Dyn.*, 39, 65
- García-Segura, G., Langer, N., Różyczka, M., & Franco, J. 1999, *ApJ*, 517, 767
- Guerrero, M., Miranda, L.F., Chu, Y-H., Rodríguez, M. & Williams, R.M., 2001, pre-print.
- Kim, J., Franco, J., Hong, S. S., Santillán, A. & Martos, M. 2000, *ApJ*, 531, 873
- Kwok, S., Su, K. Y. L., Hrivnak, B. J. 1998, *ApJ*, 501, L117

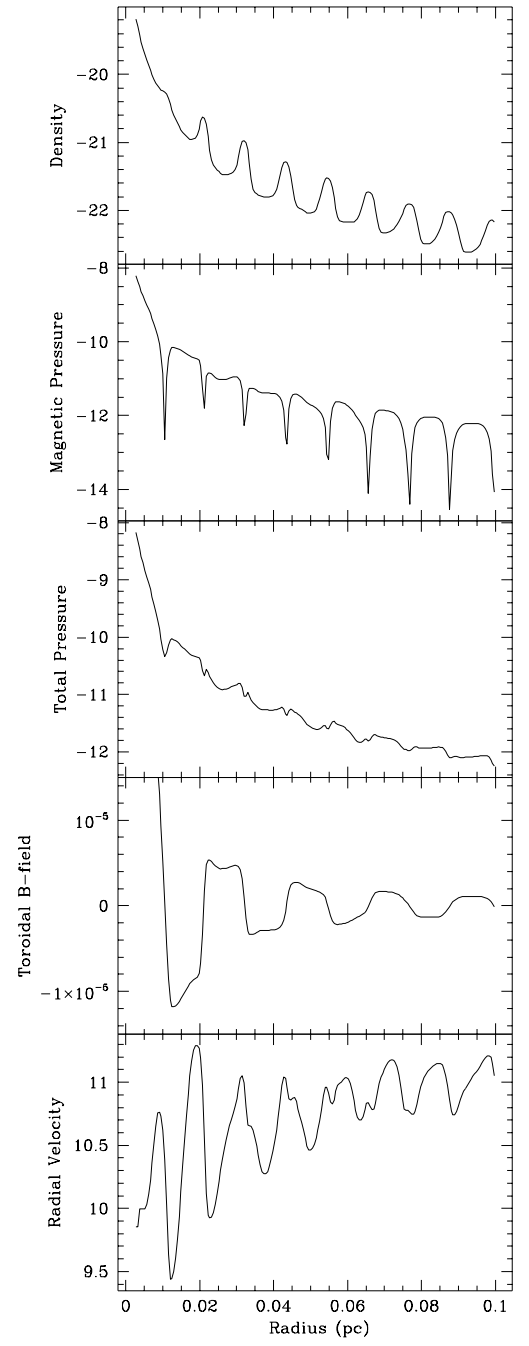
- Lazarian, A. & Vishniac, E. 1999, ApJ, 517, 700
- Mac Low, M.-M., Norman, M. L., Konigl, A., & Wardle, M. 1995, ApJ, 442, 726
- Matsumoto, R., Tajima, T., Shibata, K. & Kaising, M. 1993, ApJ, 414, 357
- Różyczka, M. & Franco, J. 1996, ApJL, 469, L127
- Sahai, R., & Nyman, L.-A. 2000, ApJ, 538, L145
- Shore, S. N. 1992, *An Introduction to Astrophysical Hydrodynamics*, (Academic Press, London)
- Smith, E.J., Tsurutani, B.T., & Rosenberg, R.L. 1978, J. Geophys. Res., 83, 717
- Soker, N. 2000, ApJ, 540, 436
- Stone, J. M. & Norman, M. L. 1992, ApJS, 80, 753
- Terzian, Y., & Hajian, A. R. 2000, *Asymmetrical Planetary Nebulae II: From Origins to Microstructures*, ed. J. H. Kastner, N. Soker, S. A. Rappaport, A.S.P. Conf. Series, 199, 33
- Wilcox, J., & Ness, N. 1965, J. Geophys. Res., 70, 1233

Figure Captions

Figure 1. Equatorial cut for the run with $\sigma = 0.01$ showing the effects of a cyclic polarity inversion of the AGB stellar magnetic field. Each density peak correspond to 1,000 yr, half of the full period. Units are in c.g.s., except for the radial velocity (km s^{-1}).

Figure 2. Emission measure of four different runs projected with a tilt of 45° from the plane of the sky. The panels correspond to: (top-left) $\sigma = 0.001$, (bottom-left) $\sigma = 0.01$, (top-right) $\sigma = 0.05$, (bottom-right) $\sigma = 0.1$. Each concentric shell correspond to 1,000 yr. Note the piled-up blobs at the polar axis for the most magnetized runs, resulting from the self-collimation of the AGB wind.

Figure 3. Comparison between the polar region of the model with $\sigma = 0.1$ (projected without tilt on the plane of the sky) (top), with figure 3 by Sahai & Nyman (2000) of He 2-90 (bottom). In their figure, the relative intensity of the jet is plotted as a function of radius showing the radial offsets of the knots from the center (thick curve: southeast jet, thin curve: northwest jet). Both plots are logarithmic in the Y axis, and linear in the X axis.



This figure "Figure2.jpg" is available in "jpg" format from:

<http://arxiv.org/ps/astro-ph/0104154v2>

